Available online at www.sciencedirect.com
ScienceDirect
Applied Catalysis B: Environmental 78 (2008) 101–111
APPLIED CATALYSIS B: ENVIRONMENTAL
www.elsevier.com/locate/apcatb

Phase change of catalysts derived from a LDH-deoxycholate intercalated compound and its impacts on NO reduction from stationary source emissions

Thakul Wongkerd, Apanee Luengnaruemitchai, Sirirat Jitkarnka *

The Petroleum and Petrochemical College, Chulalongkorn University, Chula 12, Patumwan, Bangkok 10330, Thailand

Received 5 January 2007; received in revised form 21 August 2007; accepted 11 September 2007
Available online 16 September 2007

Abstract

Deoxycholate and keggin-type polyoxometalate ($PW_{12}O_{40}$ and $SiW_{12}O_{40}$) pillared-hydrotalcite-type clay catalysts were prepared, and the effects of calcination temperature were studied on selective catalytic reduction of NO by NH_3 over excess oxygen in the reaction temperature range 150–450 °C. The results showed that over 99% N_2/N_2O selectivity was achieved at all testing temperatures for all pillared-clay catalysts. The activity of all pillared-clay catalysts increased significantly with temperature beyond 300 °C. It was found that all pillared clays had different thermal transition behaviors at various stages of calcinations temperature, which affected the SCR activity. The dehydroxylated intermediates and amorphous mixed oxide forms, whose Brønsted acid sites were still preserved after calcinations, appeared to yield high NO conversion with high N_2/N_2O selectivity. Generally, the PW_{12}-clay-derived catalysts seem to have the highest activity. Five percent Fe loading by impregnation method significantly increased activity of pillared-clay catalysts while high N_2/N_2O selectivity was maintained. Fe-loaded catalysts also showed obviously higher N_2/N_2O selectivity than the commercial catalyst; 4.4% V_2O_5–8.2% WO_3/TiO_2.

Keywords: SCR; Keggins; Polyoxometalates; Pillared clay; Hydrotalcite

1. Introduction

In the commercial SCR unit for stationary sources, vanadia-based catalysts (V_2O_5/TiO_2 catalyst) mixed with WO_3 and/or MoO_3 as promoters are used as effective catalysts. However, their toxicity due to vanadium content and high selectively toward toxic N_2O are currently the disadvantages. Several catalysts were studied in order to overcome these disadvantages. One of the most outstanding works was accomplished by Yang's group [1–8] in which cationic clays such as bentonite intercalated with titania (TiO_2–PILC) and doped with metal oxides with or without ion-exchanged elements were extensively studied as catalysts for this application. They successfully discovered that Fe–TiO_2–PILC, a vanadium-free catalyst gave the best activity and selectivity among those tested and over the commercial catalysts [2,5]. Moreover, their comprehensive study showed that pre-sulfation of the Fe–TiO_2–PILC catalyst significantly enhanced NO conversion and suppressed NH_3 oxidation in accordance with the discovery that the activity was improved by the presence of SO_2 in the feed due to the increase in surface acidity [9].

Inspired by Yang's work, for this application, clays are an interesting alternative support or catalyst to us, especially hydrotalcite-type clays, which are anionic Mg–Al-based clays reported to have high capacity of SO_x sorption [10,11], possibly due to basicity of the clay sheets. The SO_x capturing ability was presumably expected to increase the acidic part of catalyst, and then enhance the activity. They also have attractive features such as high porosity, high thermal stability and exchangeable cations [7]. Hydrotalcite-type clay is a class of layered double hydroxide (LDH) anionic clays possessing various adjustable lateral anion spacings suitable for the negatively charged such as polyoxometalate (POM) pillars, which present a wider range of thermal stability than polynuclear transition metal halides, and hydroxyl metal cations [12–15]. Kwon et al. synthesized $V_{10}O_{28}{}^{6-}$-pillared hydrotalcite (d = 11.9 Å) by direct exchange of decavanate anion ($V_{10}O_{28}{}^{6-}$) with Cl^- interlayer anion [16].

* Corresponding author. Tel.: +66 2 218 4148.
E-mail address: sirirat.j@chula.ac.th (S. Jitkarnka).

0926-3373/$ – see front matter © 2007 Elsevier B.V. All rights reserved.
doi:10.1016/j.apcatb.2007.09.008

Later, Drezdzon [13] synthesized $Mo_7O_{24}^{6-}$ (d = 12.17 Å) and $V_{10}O_{28}^{6-}$ (d = 11.8 Å)-hydrotalcite type clays starting from an organic-anion-pillared clay (terepthalate dianion-pillar) precursor, which was subsequently exchanged with appropriate POMs under mildly acidic conditions. For synthesizing POM-pillared hydrotalcite clays, Chibwe and Jones [17] was achieved by direct exposure of a calcined-hydrotalcite clay to a solution of the pillaring species, i.e., $Mo_7O_{24}^{6-}$ (d = 12.0 Å) and $V_{10}O_{28}^{6-}$ (d = 11.8 Å).

Ogawa and Asai [18] synthesized a LDH-deoxycholate intercalated compound having the gallery height (d-spacing) of 32.9 Å. Its height is sufficiently large for exchange with polyoxometalate anions such as a Keggin heteropolyanion typically represented by the formula $XM_{12}O_{40}^{x-8}$, which themselves have advantages as a catalyst in several reactions including SCR of NO [19]. Dimotakis and Pinnavaia [20] have accomplished the preparation of Keggin-type POM-pillared hydrotalcite, i.e., $H_2W_{12}O_{40}^{6-}$ (d = 14.8 Å) from terephthalate interlayer precursors. From Wang et al. [21], the POM ions with Keggin-type structure-, $PV_3W_9O_{40}$, pillared hydrotalcites ($d \sim 13.0$ Å) were successfully prepared in an aqueous one-step reaction. Several starting materials and treatment conditions were also studied in the previous works. Therefore, the LDH-deoxycholate intercalated compound hereby called "DA-Clay" was employed in this study as a precursor and support to prepare keggin-type ($PW_{12}O_{40}$ and $SiW_{12}O_{40}$) pillared-hydrotalcite-type clay catalysts for SCR of NO by ammonia. However, it was reported that hydrotalcite clays have different thermal transition behaviors in the different calcination stages [22,23]. Due to a wide range of reaction temperatures, the catalysts derived from the DA clay thus can be altered upon reaction temperature. For a catalytic application, a catalyst must be stable during the course of reaction. The knowledge on its stability toward the reaction is therefore inevitably essential.

In this contribution, the DA-clay and its two derived Keggin-intercalated clays were synthesized and used as catalysts for SCR of NO by ammonia. The impact of phase change of catalysts was investigated on activity toward the SCR reaction. The structure models of the intercalated clays at different temperatures were also presented in this work. Moreover, the effect of Fe loading on the activity was also examined. Their activity and selectivity were compared with those obtained from the commercial catalysts.

2. Experimental

2.1. Synthesis of pillared-clay catalysts

Hydrotalcite-type clays intercalated with an organic compound and two Keggin-type polyoxometalates were prepared by hydrothermal [18] and anion exchanging method [20,21] consecutively. The prepared pillared clays were calcined for 12 h, then ground and sieved to 80–120 mesh (0.125–0.178 mm) before being used as catalysts for selective catalytic reduction of nitric oxide by ammonia.

2.1.1. Deoxycholate-pillared hydrotalcite-type clay (DA-clay)

DA-clay was similarly synthesized by the method established by Ogawa and Asai [18]. 1.28 g of $Mg(OH)_2$, 0.44 g of $Al(OH)_3$, 10.76 g of deoxycholic acid and 0.1 g of NaOH were mixed in 100 ml of deionized water at room temperature with vigorous stirring (pH 8–10). Then, the suspension was transferred into an autoclave and heated at 150 °C for 48 h. The solid precipitate was collected by filtration and washed with deionized water subsequently. The product was dried at 110 °C overnight, and calcined for 12 h before being used as catalysts for SCR of NO by NH_3 and also as the precursor to prepare $PW_{12}O_{40}$-pillared hydrotalcite-type clay (PW_{12}-clay) and $SiW_{12}O_{40}$-pillared hydrotalcite-type clay (SiW_{12}-clay), using the method established by Wang et al. [21].

2.1.2. Polyoxotungstophosphate-pillared hydrotalcite-type clay (PW_{12}-clay)

A suspension of 1.0 g of dried DA-clay in 50 ml of deionized water was added to a solution containing 1.74 g of $H_3PW_{12}O_{40}$ and 0.1 g NaOH in 500 ml of deionized water (pH 8) at the temperature of 70 °C. The reaction mixture was stirred for 12 h, and then the precipitate was recovered by filtration and washed with deionized water. The product was then dried at 110 °C overnight, and calcined for 12 h before being used as catalysts for SCR of NO by NH_3.

2.1.3. Polyoxotungstosilicate-pillared hydrotalcite-type clay (SiW_{12}-clay)

A suspension of 1.0 g of dried DA-clay in 50 ml of deionized water was added to a solution containing 1.31 g $H_4SiW_{12}O_{40}$ and 0.15 g NaOH in 500 ml of deionized water (pH 8) at the temperature of 70 °C. The reaction mixture was stirred for 12 h and then the precipitate was recovered by filtration and washed with deionized water. The catalyst was dried at 110 °C overnight, and calcined for 12 h before being used as catalysts for SCR of NO by NH_3.

2.1.4. Fe-loaded pillared-clay catalysts

To study the promoting effects of iron to pillared clays, iron was loaded on the pillared-clay catalysts by an impregnation method. Appropriate amount of ferric nitrate ($Fe(NO_3)_3 \cdot 9H_2O$) solution was impregnated into the calcined pillared clays to obtain 5%wt of Fe. After that, the solid were dried at 110 °C for overnight, and calcined for 12 h before being used as catalysts for SCR of NO by NH_3.

2.2. Catalyst characterization

The changes in characteristics of pillared clay such as phase transition, morphology, and surface area upon temperature were studied by several techniques, i.e., TGA, XRD, SEM and BET. The prepared catalysts were characterized by a DuPont TGA 2950 Thermogravimetric analyzer. The specimen was heated up from 30 to 700 °C with a rate of 10 °C/min, followed by cooling down to 30 °C with a rate of 10 °C/min. XRD was

performed on a Rigagu X-ray diffractometer (RINT-2200) with Cu Kα (1.5406 Å) radiation was used with a divergence slit = 0.5°, scattering slit = 0.5°, and receiving slit = 0.15 mm. The samples were loaded on a sample holder with a depth of 1 mm. XRD patterns were recorded in the range 2θ = 1.2–90° in 5°/min step-scan. JCPDS database was employed on identification of phases. Autosorb-1 Gas sorption system (Quantachrome Coorporation) was used to examine BET surface area, and average pore volume and diameter of samples.

2.3. Catalytic activity testing

The catalytic activity of selective catalytic reduction of NO_x with ammonia was carried out at atmospheric pressure, using the experimental setup as similarly shown in Yang's work [5–9]. 0.2 g of catalyst was placed with glass wool in the fixed-bed flow reactor. The sizes of catalyst powder were in the range of 0.125–0.175 mm (80–120 mesh), which were small enough to ensure that there was no internal diffusion limitation. Temperature of the catalyst bed was examined and controlled by PID controller equipped with K-type thermocouple (Yogohama, Model UP27). The reactant mixture consisted of 1000 ppm NO, 1000 ppm NH_3, 2% O_2, and balanced with He. The total flow rate was 500 ml/min, which can be converted to the GHSV of $1.13 \times 10^5\ h^{-1}$. The mixture was passed separately to Hewlett Packard 3365 series II Chemstation with 13× molecular sieve column for analyzing O_2 and N_2 concentration. Moreover, it also passed through a bubbler for ammonia removal in order to avoid the ammonia oxidation in the converter of NO/NO_x analyzer, and then, to the Chemiluminescence $NO–NO_2–NO_x$ analyzer (Model CLD 700 EL) from ECO Physics in order to determine the concentration of nitric oxide (NO), and nitrogen dioxide (NO_2). Nitrous oxide was calculated from mass balance.

3. Results and discussion

3.1. Characteristics of pillared-clay catalysts upon temperature changes

The transition weight loss of pillared clays upon temperature was investigated by TGA technique. The TGA and DTG plots are shown in Fig. 1. The weight loss behavior of all pillared clays appears in three zones. In the first zone, water located at surface and between interlayer of clay sheet was lost when the temperature was increased toward and beyond its boiling point. This first transition appears up to 300 °C. The second transition is started between 300 and 500 °C, and the third transition is beyond 500 °C. In the second zones beyond the first transition, the DA-clay starts to lose one by one their two interlayers of deoxycholate anions and hydroxy groups while the PW_{12}-clay and $SiW_{12}O_{40}$-clay start to lose their layer structure until the third transition at 500 °C where all clays might have completely lost the layer structure and become mixed oxides.

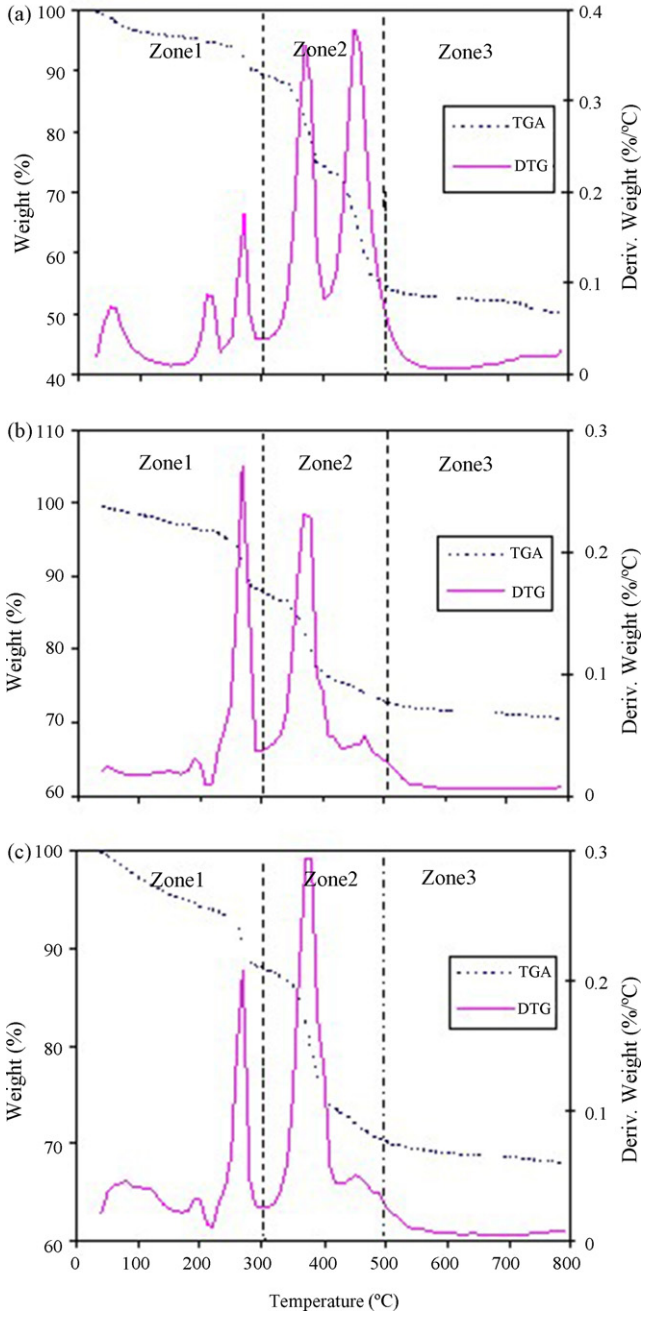

Fig. 1. TGA and DTG of (a) DA-clay, (b) PW_{12}-clay, and (c) $SiW_{12}O_{40}$-clay.

XRD patterns of the pillared-clay-based catalysts after drying and calcination are shown in Fig. 2. The (0 0 1) plane peak of dry DA-clay occurs at the 2θ angle of 2.65°, which has the *d*-spacing value of 32.90 Å. These values agree well with the data reported in Ogawa and Asai [18], which stated that the intercalated deoxycholate formed as a bilayer in the interlayer space where the carboxylate was believed to orient to the surface of the cationic brucite-like sheet. The (0 0 1) plane peak of dried PW_{12}-clay and SiW_{12}-clay appears at the 2θ angle of 6.02°, which has the *d*-spacing value of 14.67 Å. The XRD pattern of dry pillared clays also shows a $Mg(OH)_2$ phase at the 2θ angle of 18.36° and 38.04°. When the pillared clays were

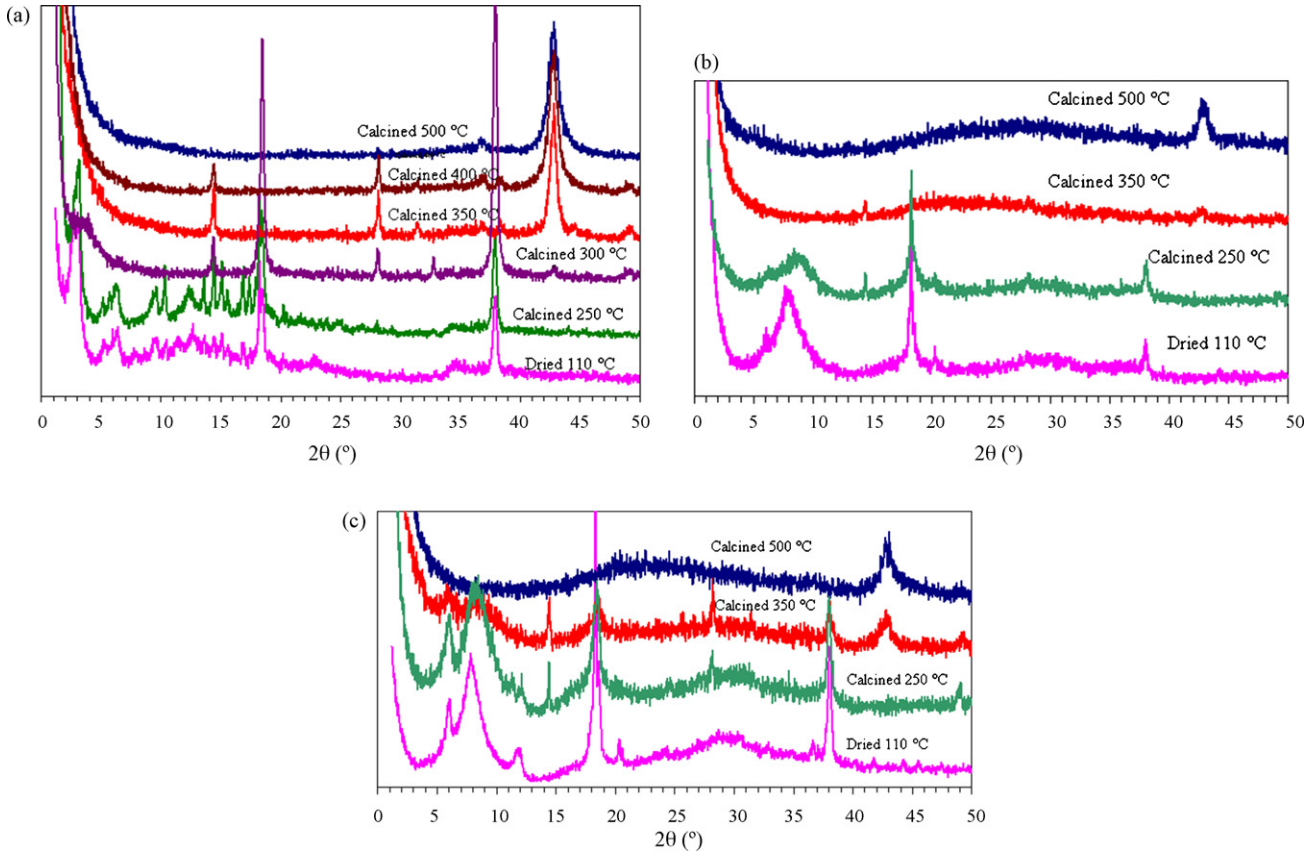

Fig. 2. XRD patterns of (a) DA-clay, (b) $PW_{12}O_{40}$-clay, and (c) SiW_{12}-clay at different calcination temperatures.

calcined at 250 °C, most of the peaks still occur at the same 2θ angle, which means the structure of pillared clay did not change significantly at this temperature. The diffraction peak of DA-clay calcined at 300 °C shows the flat plane peak at the 2θ angle of 3.78°, which has the *d*-spacing value of 23.36 Å. At this temperature, a magnesium oxide (MgO) phase is observed at the 2θ angle of 42.82° in addition to $Mg(OH)_2$ phase, indicating the initial loss of some deoxycholate ions, and layer structure such as hydroxy groups at this temperature. After the clay was calcined at 350 °C and 400 °C, sharp peak of MgO phase is observed, indicating the progressive loss of deoxycholate ions and layer structure. Similar to the DA-clay, the plane peak of PW_{12}-clay disappeared when it was calcined at 350 °C, and a magnesium oxide (MgO) phase was also observed at this temperature but less than the DA-clay. Major characteristic peaks of SiW_{12}-clay still remained at 350 °C (See Fig. 2c), indicating that this pillared clay might have the highest thermal stability. However, a magnesium oxide (MgO) phase was also formed as similarly as in the DA-clay and PW_{12}-clay cases. After all pillared clays were calcined at 500 °C, most of the peaks disappeared, which indicates the complete loss of deoxycholate ions in DA-clay and layer structure of all pillared clays, and the transformation of clay structure to amorphous mixed oxides (MgO and Mg–Al–O). These observations agree well with the TGA results.

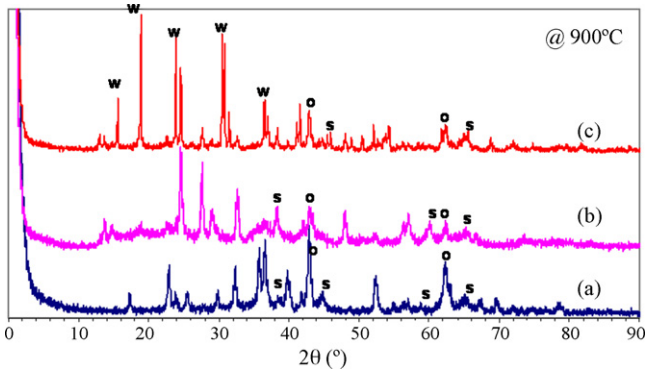

Fig. 3. XRD patterns of pillared clays calcined at 900 °C—(a) DA-clay, (b) $PW_{12}O_{40}$-clay, and (c) SiW_{12}-clay: (w) $Mg(OH)_2$ phase, (o) MgO phase, and (s) spinel phase.

After all pillared clays were calcined at 900 °C, higher crystallinity material was observed. The XRD patterns of these products are shown in Fig. 3. It consists of sharp peaks of MgO and some trace of $MgAl_2O_4$ (spinel), indicating the change from the amorphous Mg–Al–O mixed oxide into $MgAl_2O_4$. Moreover, some peaks of $MgWO_4$ phase occur on the SiW_{12}-clay, indicating that the Keggin interlayer ions in this pillared clay formed the mixed oxide with the element in the clay sheets. This observation agrees with the evolution of general hydrotalcite clay that had been reported elsewhere [24,25].

The surface morphology of dried and calcined pillared-clay catalysts is shown in Figs. 4–6. All dried pillared clays were

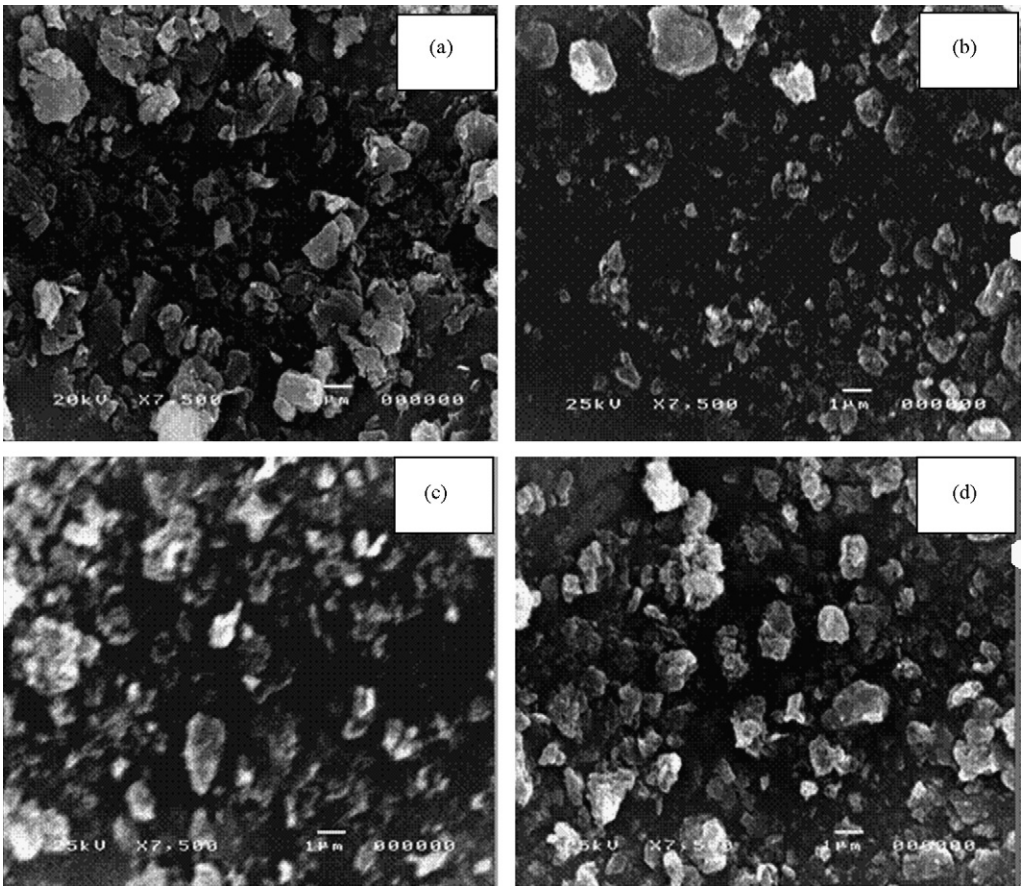

Fig. 4. Scanning electron micrographs at 7500× magnification of (a) dried DA-clay, (b) DA-clay calcined at 350 °C, (c) DA-clay calcined at 500 °C, and (d) DA-clay calcined at 900 °C.

found in cornflake shape of clay morphology similar to what was depicted in Ogawa and Asai [18]. After all pillared clays were calcined at 350 and 500 °C, similar amorphous surface morphology was observed. Then, higher crytallinity was obtained after the materials were further calcined at 900 °C due to the formation of mixed oxides as described in the TGA and XRD parts. The information observed in the SEM images therefore conformed to those described in the TGA and XRD parts.

Yong et al. [23] studied the effect of temperature on CO_2 adsorption capacity of commercial hydrotalcite-type compounds (HTlcs). The compounds had different CO_2 capacity, which depended upon the evolution of the HTlcs structures, deforming upon temperature change. Accompanied with the discoveries by Bellolotto et al. [26], they proposed the structure models illustrating the compound in three different stages of calcination: (a) the starting HTlcs, (b) the dehydrated intermediate, and (c) the decomposed material. These stages are analogous to those observed by the TGA and XRD in our cases. Therefore, adapted from Yong et al. [23], the structure models of the DA Clay, and PW_{12}-Clay or SiW_{12}-Clay at different calcination temperatures are illustrated in Figs. 7 and 8. The evolution of structures can be divided into five stages: (a) the starting compound (dry samples), (b) dehydrated intermediate (calcined at 250 °C), (c) dehydroxylated intermediate (calcined at 350 °C), (d) amorphous mixed oxides (calcined at 500 °C), and (e) highly crystalline mixed oxides (calcined at 900 °C).

BET technique was employed for determining BET surface area, pore volume, and average pore diameter of pillared-clay catalysts calcined at 350 and 500 °C. The results are tabulated in Table 1. The surface area of these catalysts is in the range of 48.7–125.6 m^2/g. The pillared clays calcined at 350 °C have the surface area of around 48.7–79.0 m^2/g. After calcination at 500 °C, the surface area of about 107.9–125.6 m^2/g was obtained, which is much larger than those calcined at 350 °C. The BET surface area of all pillared-clay catalysts exhibited in the same trend, indicating the deformation of layer structure into more amorphous phases (as observed by the TGA and XRD results) might result in the increase in surface area. The pore volume of pillared-clay catalysts is between 0.14 and 0.26 cm^3/g, and the average pore diameter is in the range of 82.7–127 Å.

3.2. SCR catalytic activity of pillared-clay catalysts

3.2.1. Effect of phase changes on SCR activity

The effects of phase changes to the activity and selectivity of pillared-clay catalysts were examined in this section. According to the five stages depicted in the structure models, only the

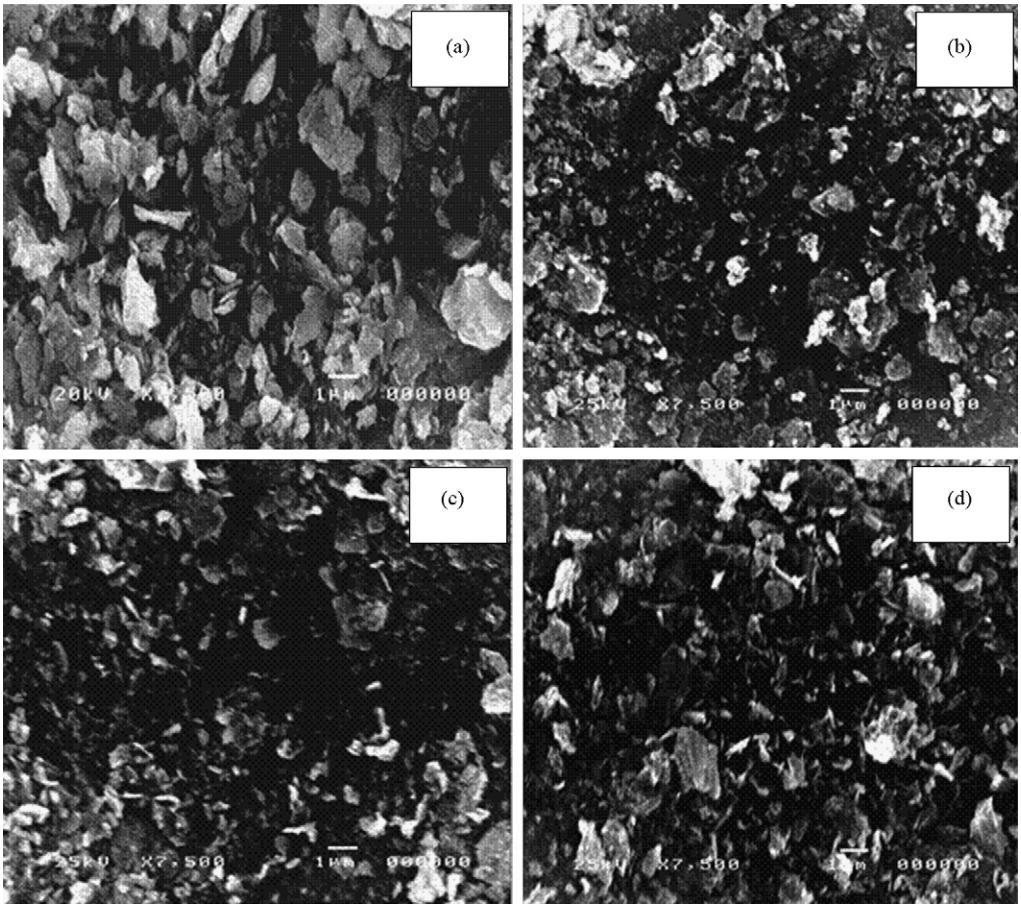

Fig. 5. Scanning electron micrographs at 7500× magnification of (a) dried PW_{12}-clay, (b) PW_{12}-clay calcined at 350 °C, (c) PW_{12}-clay calcined at 500 °C, and (d) PW_{12}-clay calcined at 900 °C.

last four stages were selected for catalytic activity testing: (i) pillared-clay catalysts calcined at 250 °C (denoted DA-clay250, PW_{12}-clay250, and SiW_{12}-clay250), (ii) pillared-clay catalysts calcined at 350 °C (denoted DA-clay350, PW_{12}-clay350, and SiW_{12}-clay350), (iii) pillared-clay catalysts calcined at 500 °C (denoted DA-clay500, PW_{12}-clay500, and SiW_{12}-clay500), and (iv) pillared-clay catalysts calcined at 900 °C (denoted DA-clay900, PW_{12}-clay900, and SiW_{12}-clay900). Since the range of testing temperature was 150–450 °C, the dry clay was not selected because it cannot even maintain its form at the minimum testing temperature. Note here that all selected clay catalysts were tested for their activity at the temperatures up to their calcination temperatures. The activity testing results are shown in Tables 2–5. Around 99.1–99.9% N_2/N_2O selectivity was achieved on all pillared-clay-based catalysts, indicating there is no or little oxidation of NH_3 forming N_2O over these catalysts in all testing temperatures [27].

The NO conversion obtained from the pillared-clay catalysts calcined 250 °C is about 2% (the DA-clay250) to around 6% (for all others) at all testing temperatures (Table 2). At this calcination temperature, all pillared clays dehydrated, but the dry clays still retained a layer structures and interlayer ions. Mostly, SCR activity of this phase might be contributed from interlayer ions between layers of each clay. The organic deoxycholate anions in the DA-clay250 layers contribute to the lowest activity even though they give the highest *d*-spacing to the clays. All pillared-clay catalysts calcined at 350 °C give about 6% NO conversion at all testing temperatures. The activity of DA-clay350 catalyst significantly increases as compared to the DA-clay250 while the activity of the others is almost the same as the ones calcined at 250 °C (Table 3). As stated in Section 3.1, the interlayer, deoxycholate ions of DA-clay were removed at the calcination temperature of 350 °C, causing some changes on layer structure. Moreover, dehydroxylation process causes the formation of MgO, and Mg–Al–O. It has been accepted that the Brønsted acidity is the most important property of catalyst for SCR of NO by NH_3 [2,5,6,8]. The Mg–Al–O group is the source of Brønsted acidity in all clay catalysts; therefore, it promotes the SCR reaction and increases the activity of all catalysts, especially that of the DA-clay one.

The pillared-clay catalysts calcined at 500 °C, whose layer structure was believed to collapse at this temperature, gave significantly higher activity than the others at all testing temperatures. About 11–14% NO conversion was obtained at 150–250 °C for all pillared-clay catalysts, and the activity of all catalysts increased significantly beyond the reaction

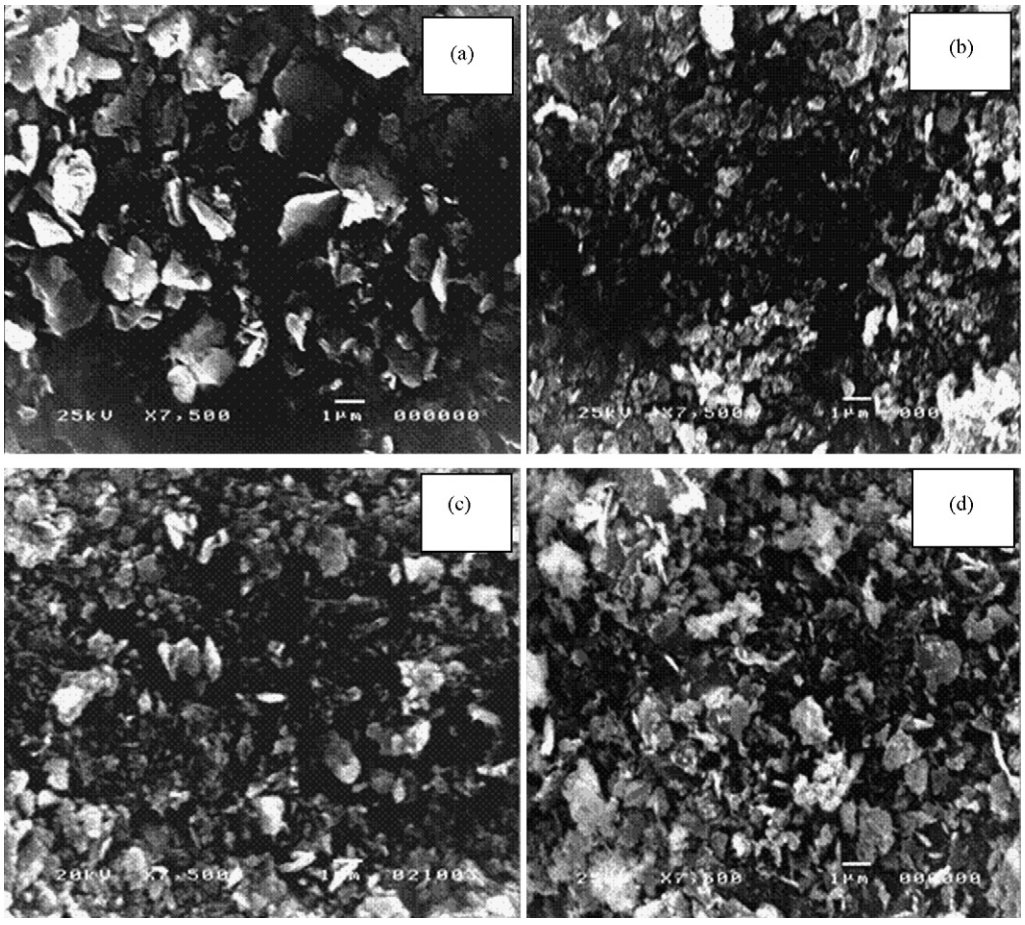

Fig. 6. Scanning electron micrographs at 7500× magnification of (a) dried SiW_{12}-clay, (b) SiW_{12}-clay calcined at 350 °C, (c) SiW_{12}-clay calcined at 500 °C, and (d) SiW_{12}-clay calcined at 900 °C.

temperature of 300 °C, and reached the highest at 450 °C. The PW_{12}-clay500 gave the highest NO conversion of 31.2%. The DA-clay500 gave 20% NO conversion, and the SiW_{12}-clay500 showed 26% NO conversion. The activity of all catalysts calcined at 500 °C is reported in Table 4. The number of Brønsted acid sites may be possibly increased by increasing the formation of Mg–Al–O groups from dehydroxylation process at this calcination temperature. Moreover, surface area and pore volume were increased by the deformation of layer structure (as stated in Section 3.1). Thus, the activity of this phase was much higher than the previous two stages. In addition, new compounds of keggins occurring at this temperature may possibly promote the activity on the PW_{12}-clay500 and SiW_{12}-clay500 at high reaction temperatures (300–450 °C). At calcination temperature of 900 °C, the result shows lower activity of all catalysts than that of those calcined at 500 °C. The NO conversion of DA-clay900 and SiW_{12}-clay900 is in the range of 7–10% at low reaction temperatures (150–300 °C), and the PW_{12}-clay900 gave the highest activity of 26% at 450 °C. New phases such as spinel or $MgWO_4$ therefore can suppress the activity, and calcination at high temperature can also decrease the Brønsted acidity on all clay catalysts, and then decrease the activity. The evolution of the pillared-clay structure described above is illustrated in Figs. 7 and 8.

In summary, stability of clay catalysts toward temperature change is an important parameter in making decision on using the catalysts in the SCR of NO. In general, the amorphous mixed oxide stage (calcined at 500 °C) seem to be the best forms among the other four stages of catalysts derived from the hydrotalcite clay for the SCR of NO by ammonia.

3.2.2. *Promoting effect of Fe*

Iron was loaded on pillared-clay catalysts calcined at 500 °C in order to determine the promoting effect of Fe. It was found that 5%Fe loading significantly increased NO conversion at temperature beyond 350 °C. The highest 40% NO conversion was achieved at 450 °C on the Fe–PW_{12}–clay catalyst (Table 6). Most catalysts exhibited more than 99% N_2/N_2O selectivity at all testing temperatures, indicating no or little amount of N_2O was formed on Fe-loaded clay catalysts. Cheng et al. [2] suggested that both Fe=O and Fe–OH, which are the Brønsted acid sites Fe_2O_3/Cr_2O_3 on TiO_2 catalyst were necessary for SCR reaction. The mechanism had been also illustrated. Therefore, it is reasonable to suggest that Fe-loading increases the Brønsted acidity of pillared-clay catalysts, and then enhances the activity.

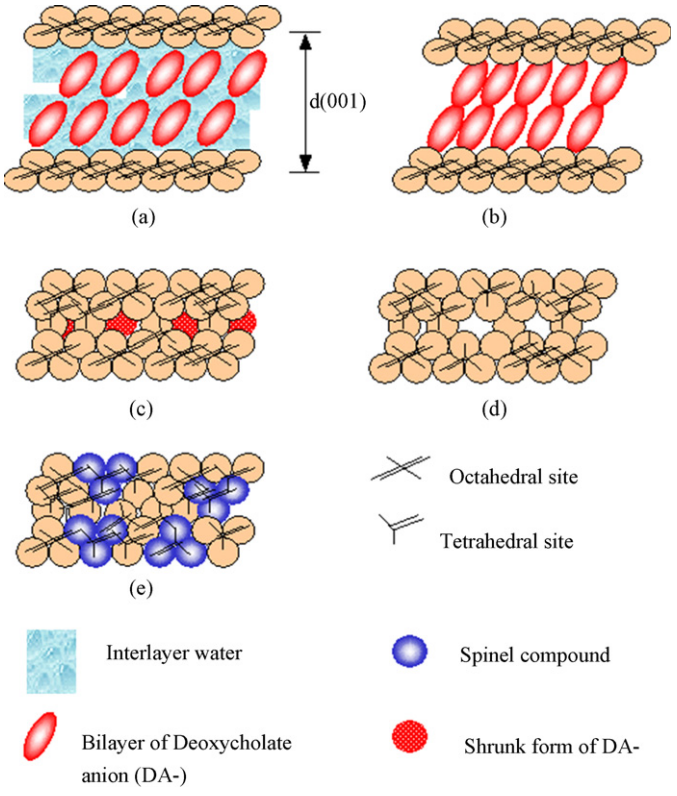

Fig. 7. Structure models of DA-clay at different temperatures: (a) dried DA-clay, (b) dehydrated intermediate (calcined at 250 °C), (c) dehydroxylated intermediate (calcined at 350 °C), (d) amorphous mixed oxides (calcined at 500 °C), and (e) highly crystalline mixed oxides (calcined at 900 °C; spinel and MgO included): adapted from [23,26].

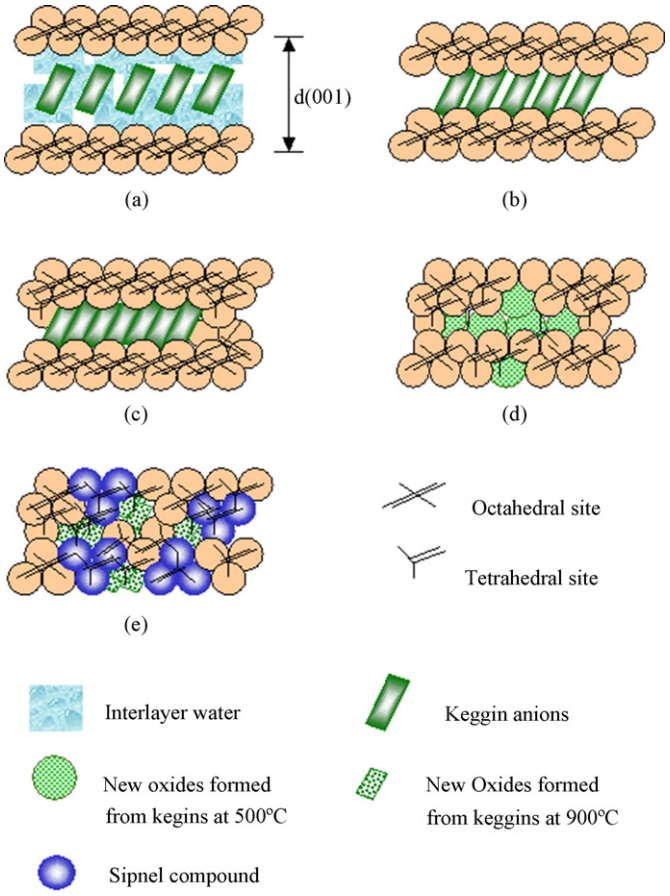

Fig. 8. Structure models of keggin-clays (PW_{12}-clay or SiW_{12}-clay) at different temperatures: (a) dried clays, (b) dehydrated intermediate (calcined at 250 °C), (c) dehydroxylated intermediate (calcined at 350 °C), (d) amorphous mixed oxides (calcined at 500 °C), and (e) highly crystalline mixed oxides (calcined at 900 °C; other mixed oxides such as spinel, $MgWO_4$ and MgO included): adapted from [23,26].

3.2.3. Comparison between the clay-based catalysts and commercial catalyst

The NO conversion and N_2/N_2O selectivity data of the commercial catalyst (4.4% V_2O_5 + 8.2% WO_3/TiO_2) were taken from Long and Yang [5] for comparison. The SCR activity results are shown in Fig. 9 and tabulated in Table 7. By comparison, the commercial catalyst gave higher NO conversion at all testing temperatures. However, NO conversion of the commercial catalyst decreased after passing though a maximum at 375 °C. In addition, the N_2/N_2O selectivity for the commercial catalyst decreased more rapidly with increasing temperature of over 350 °C. This observation indicated that NH_3 oxidation by O_2 occurred on the commercial catalyst resulting in the decrease in NO conversion at high temperatures [27]. However, on the other hand, over 99% N_2/N_2O selectivity

Table 1
BET characterization

Catalyst	Surface area (m^2/g)	Pore volume (cm^3/g)	Average pore diameter (Å)
1. DA-clay			
Calcined 350 °C	48.71	0.14	114.60
Calcined 500 °C	125.60	0.26	82.68
2. PW_{12}-clay			
Calcined 350 °C	78.99	0.25	127.40
Calcined 500 °C	107.90	0.24	90.53
3. SiW_{12}-clay			
Calcined 350 °C	77.87	0.17	86.52
Calcined 500 °C	116.30	0.18	109.2

Table 2
SCR activity of pillared-clay-based catalysts calcined at 250 °C

Catalyst	Reaction temperature (°C)	NO conversion (%)	Selectivity (%)		
			N_2[a]	N_2O[b]	NO_2
DA-clay250	150	1.6	99.8	0.2	0
	200	1.5	99.8	0.2	0
	250	2.2	99.8	0.2	0
PW_{12}-clay250	150	5.6	99.4	0.6	0
	200	5.1	99.6	0.4	0
	250	6.2	99.9	0.1	0
SiW_{12}-clay250	150	5.9	99.9	0.1	0
	200	6.3	99.7	0.3	0
	250	6.3	99.8	0.2	0

[a] N_2/N_2O selectivity.
[b] N_2O/N_2 selectivity.

Table 3
SCR activity of pillared-clay-based catalysts calcined at 350 °C

Catalyst	Reaction temperature (°C)	NO conversion (%)	Selectivity (%)		
			N_2[a]	N_2O[b]	NO_2
DA-clay350	150	6.2	99.8	0.2	0
	200	6.2	99.5	0.5	0
	250	6.2	99.7	0.3	0
	300	6.6	99.7	0.3	0
	350	6.6	99.5	0.5	0
PW_{12}-clay350	150	6.1	99.9	0.1	0
	200	6.2	99.9	0.1	0
	250	6.3	99.7	0.3	0
	300	6.0	99.9	0.1	0
	350	6.2	99.9	0.1	0
SiW_{12}-clay350	150	6.2	99.6	0.4	0
	200	6.3	99.4	0.6	0
	250	6.2	99.8	0.2	0
	300	6.3	99.7	0.3	0
	350	6.7	99.9	0.1	0

[a] N_2/N_2O selectivity.
[b] N_2O/N_2 selectivity.

was achieved over all Fe-pillared-clay catalysts at all testing temperatures.

Although the commercial catalyst gave high NO conversion, another toxic gas N_2O was produced over this catalyst at the commercially SCR operating temperature of 350–450 °C. Therefore, the clay-based catalysts have high potential to be developed for using as catalysts in SCR process. Although their conversion may be lower than the commercial catalyst, the selectivity at operating temperatures is much higher. Higher amount of catalyst may be needed to obtain higher conversion with maintained high selectivity.

Table 4
SCR activity of pillared-clay-based catalysts calcined at 500 °C

Catalyst	Reaction temperature (°C)	NO conversion (%)	Selectivity (%)		
			N_2[a]	N_2O[b]	NO_2
DA-clay500	150	10.3	99.7	0.3	0
	200	11.8	99.8	0.2	0
	250	11.8	99.8	0.2	0
	300	14.7	99.6	0.4	0
	350	16.2	99.8	0.2	0
	400	19.1	99.4	0.6	0
	450	20.6	99.6	0.4	0
PW_{12}-clay500	150	11.8	99.7	0.3	0
	200	13.2	99.7	0.3	0
	250	13.4	99.8	0.2	0
	300	15.0	99.7	0.3	0
	350	19.0	99.6	0.4	0
	400	26.5	99.4	0.6	0
	450	31.2	99.4	0.6	0
SiW_{12}-clay500	150	10.3	99.5	0.5	0
	200	11.8	99.4	0.6	0
	250	11.8	99.4	0.6	0
	300	17.9	99.8	0.2	0
	350	18.5	99.3	0.7	0
	400	22.1	99.4	0.6	0
	450	26.5	99.3	0.7	0

[a] N_2/N_2O selectivity.
[b] N_2O/N_2 selectivity.

Table 5
SCR activity of pillared-clay-based catalysts calcined at 900 °C

Catalyst	Reaction temperature (°C)	NO conversion (%)	Selectivity (%)		
			N_2[a]	N_2O[b]	NO_2
DA-clay900	150	5.7	99.9	0.1	0
	200	7.6	99.6	0.4	0
	250	7.6	99.7	0.3	0
	300	8.7	99.5	0.5	0
	350	9.4	99.8	0.2	0
	400	11.8	99.6	0.4	0
	450	15.1	99.9	0.1	0
PW_{12}-clay900	150	13.2	99.4	0.6	0
	200	13.2	99.4	0.6	0
	250	14.7	99.5	0.5	0
	300	16.3	99.8	0.2	0
	350	17.6	99.6	0.4	0
	400	20.7	99.2	0.8	0
	450	26.0	99.4	0.6	0
SiW_{12}-clay900	150	7.1	99.4	0.6	0
	200	7.1	99.9	0.1	0
	250	8.3	99.7	0.3	0
	300	9.9	99.8	0.2	0
	350	10.6	99.2	0.8	0
	400	15.9	99.1	0.9	0
	450	17.3	99.1	0.9	0

[a] N_2/N_2O selectivity.
[b] N_2O/N_2 selectivity.

Table 6
SCR activity of Fe-loaded pillared-clay-based catalysts calcined at 500 °C

Catalyst	Reaction temperature (°C)	NO conversion (%)	Selectivity (%)		
			N_2[a]	N_2O[b]	NO_2
Fe-DA-clay	150	11.8	99.7	0.3	0
	200	12.4	99.4	0.6	0
	250	12.4	99.7	0.3	0
	300	14.7	99.7	0.3	0
	350	19.1	99.6	0.4	0
	400	26.5	99.5	0.5	0
	450	30.9	99.2	0.8	0
Fe-PW_{12}-clay	150	11.8	99.8	0.2	0
	200	13.2	99.8	0.2	0
	250	13.7	99.8	0.2	0
	300	15.7	99.5	0.5	0
	350	20.6	99.6	0.4	0
	400	30.9	99.7	0.3	0
	450	39.9	99.4	0.6	0
Fe-SiW_{12}-clay	150	11.8	99.4	0.6	0
	200	11.8	99.9	0.1	0
	250	11.8	99.5	0.5	0
	300	18.2	99.7	0.3	0
	350	19.1	99.7	0.3	0
	400	25.1	99.6	0.4	0
	450	29.4	99.4	0.6	0

[a] N_2/N_2O selectivity.
[b] N_2O/N_2 selectivity.

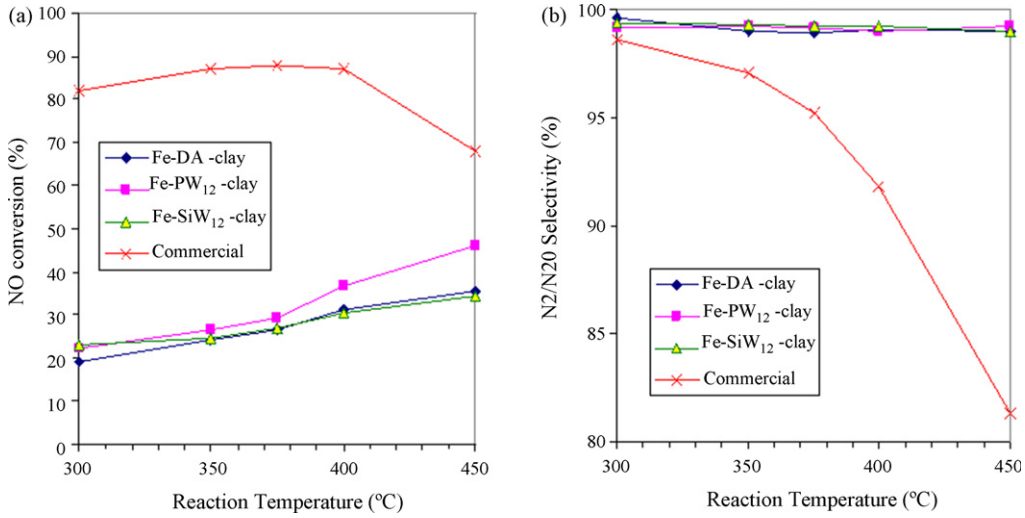

Fig. 9. SCR activity: (a) NO conversion, and (b) N_2/N_2O selectivity of the commercial catalyst and Fe-pillared-clay catalysts.

Table 7
SCR activity comparison between the commercial catalyst and Fe-pillared-clay catalysts

Catalyst	Reaction temperature (°C)	NO conversion (%)	Selectivity (%)		
			N_2[a]	N_2O[b]	NO_2
Fe-DA-clay[c]	300	19.3	99.6	0.4	0
	350	24.1	99.0	1.0	0
	375	26.5	99.0	1.0	0
	400	31.2	99.1	0.9	0
	450	35.6	99.0	1.0	0
Fe-PW_{12}-clay[c]	300	22.4	99.1	0.9	0
	350	26.6	99.3	0.7	0
	375	29.1	99.2	0.8	0
	400	36.9	99.0	1.0	0
	450	46.3	99.2	0.8	0
Fe-SiW_{12}-clay[c]	300	23.1	99.4	0.6	0
	350	24.6	99.3	0.7	0
	375	26.9	99.3	0.7	0
	400	30.4	99.3	0.7	0
	450	34.3	99.0	1.0	0
4.4% V_2O_5 + 8.2% WO_3/TiO_2[d]	300	82.0	98.6	1.4	–
	350	87.0	97.1	2.9	–
	375	88.0	95.2	4.8	–
	400	87.0	91.8	8.2	–
	450	68.0	81.3	18.7	–

[a] N_2/N_2O selectivity0.2 g catalyst was used.
[b] N_2O/N_2 selectivity.
[c] 0.2 g catalyst was used.
[d] Data from Long and Yang [5].

4. Conclusions

Upon calcination, the structures of clay catalysts can be divided into five stages: (a) the starting compound (dry samples), (b) dehydrated intermediate (calcined at 250 °C), (c) dehydroxylated intermediate (calcined at 350 °C), (d) amorphous mixed oxides (calcined at 500 °C), and (e) highly crystalline mixed oxides (calcined at 900 °C). The last four stages of pillared hydrotalcite-type clays were studied for their activity on SCR of NO using NH_3 as a reducing agent at the temperatures of 150–450 °C. As a result, all clay catalysts gave over 99% N_2/N_2O selectivity at all testing temperatures. The activity significantly increased with reaction temperature beyond 300 °C. Different thermal transition behaviors in the different stages of calcination temperatures apparently affected the SCR activity of all clay catalysts. The results showed the pillared-clay catalysts calcined at 500 °C gave higher activity than the others, and the PW_{12}-clay catalyst had the highest activity. The dehydroxylated intermediate and the mixed oxides, therefore, appeared to yield high NO conversion with maintaining high selectivity. In general, it can be concluded that catalysts at stages where Brønsted acid sites are created or still preserved upon temperature change give high NO conversion with high selectivity. Five percent Fe loading by impregnation method significantly increased the activity of pillared-clay catalysts while N_2/N_2O selectivity was maintained. Fe-loaded catalysts also showed obviously higher N_2/N_2O selectivity over the commercial catalyst; 4.4% V_2O_5–8.2% WO_3/TiO_2.

Acknowledgements

This research work was supported by Annual Government Fund, Fiscal years of 2004–2005 and partially supported by the Postgraduate Education and Research Program in Petroleum and Petrochemical Technology (under the ADB Fund). The authors would like to thank Prof. Ralph T. Yang for his valuable comments.

References

[1] R.T. Yang, W.B. Li, J. Catal. 155 (1995) 414–417.
[2] L.S. Cheng, R.T. Yang, N. Chen, J. Catal. 164 (1996) 70–81.
[3] W. Li, M. Sirilumpen, R.T. Yang, Appl. Catal. B: Environ. 11 (1997) 347–363.
[4] R.T. Yang, N. Tharapppiwattananon, R.Q. Long, Appl. Catal. B: Environ. 19 (1998) 289–304.
[5] R.Q. Long, R.T. Yang, J. Catal. 186 (1999) 254–268.

[6] R.Q. Long, R.T. Yang, Appl. Catal. B: Environ. 24 (2000) 13–21.
[7] R.Q. Long, R.T. Yang, Appl. Catal. B: Environ. 27 (2000) 87–95.
[8] R.Q. Long, R.T. Yang, J. Catal. 196 (2000) 73–85.
[9] R.Q. Long, M.T. Chang, R.T. Yang, Appl. Catal. B: Environ. 33 (2001) 97–107.
[10] A.A. Vierheilig, US Patent 6,028,023, February 22 (2000).
[11] E.W. Alber, H.W. Burkhead, US Patent 6,156,696 December 5 (2000).
[12] T. Kwon, T.J. Pinnavaia, Chem. Mater. 1 (1989) 381–438.
[13] M.A. Drezdzon, Inorg. Chem. 27 (1988) 4628–4632.
[14] A. Bhuttacharyya, D.B. Hall, Inorg. Chem. 31 (1992) 3869–3870.
[15] L. Li, S. Ma, X. Liu, Y. Yue, J. Huii, R. Xu, Y. Bao, J. Rocha, Chem. Mater. 8 (1996) 204–208.
[16] T. Kwon, G.A. Tsigdinos, T.J. Pinnavaia, J. Am. Chem. Soc. 110 (1988) 3653–3654.
[17] K. Chibwe, W. Jones, Chem. Mater. 1 (1989) 489–490.
[18] M. Ogawa, S. Asai, Chem. Mater. 12 (2000) 3253–3255.
[19] I.V. Kozhevnikov, Chem. Rev. 98 (1998) 171–198.
[20] E.D. Dimotakis, T.J. Pinnavaia, Inorg. Chem. 29 (1990) 2393–2394.
[21] J.W. Wang, Y. Tian, R. Wang, A. Clearfield, Chem. Mater. 4 (1992) 1276–1282.
[22] J. Shen, J.M. Kobe, Y. Chen, J.A. Dumesic, Langmuir 10 (1994) 3902–3908.
[23] Z. Yong, V. Meta, A.E. Rodrigues, Ind. Eng. Chem. Res. 40 (2001) 204–209.
[24] National institute for resources and environment, NIRE annual report (1995).
[25] National institute for resources and environment, NIRE annual report (1999).
[26] M. Bellolotto, B. Rebours, O. Clause, J. Lynch, D. Bazin, E. Elkaim, J. Phys. Chem. 100 (1996) 8535–8542.
[27] R.T. Yang, J.P. Chen, E.S. Kikkinides, L.S. Cheng, Ind. Eng. Chem. Res. 31 (1992) 1440–1445.